Study on spatial distribution of crop residue burning and $PM_{2.5}$ change in China

Shuai Yin [a]*, Xiufeng Wang [b], Yi Xiao [c], Hiroshi Tani [b], Guosheng Zhong [a] and Zhongyi Sun [a]

[a] Graduate School of Agriculture, Hokkaido University, Sapporo 0608589, Japan ; yinshuai@env.agr.hokudai.ac.jp (S.Y.); zhgs@env.agr.hokudai.ac.jp (G.Z.); sunzy025@env.agr.hokudai.ac.jp (Z.S.)

[b] Research Faculty of Agriculture, Hokkaido University, Sapporo 0608589, Japan; wang@env.agr.hokudai.ac.jp (X.W.); tani@env.agr.hokudai.ac.jp (H.T.)

[c] College of Tourism and Land Resources, Chongqing Technology and Business University, Chongqing 400067, China; xiaoyi999999@yeah.net

Abstract: With China as the study area, MODIS MOD14A1 and MCD12Q1 products were used to derive daily crop residue burning spots from 2014, 2015. After vectorization of crop residue burning pixels and with the use of fishnet, burning density distribution maps were eventually completed. Meanwhile, the daily air quality data from 150 cities in 2014 and 285 cities in 2015 were used to obtain daily and monthly $PM_{2.5}$ distribution maps with the Kriging interpolation. The results indicate that crop residue burning occurs in a seasonal pattern, and its spatial distribution is closely related to farming activities. The annual $PM_{2.5}$ in China decreased 11.81% from 2014 to 2015, and the distribution of $PM_{2.5}$ in China's east and north is always higher than in China's west and south. Furthermore, the changes in $PM_{2.5}$ exhibit a hysteresis after crop residue burning in summer and autumn-winter. Regarding summer crop residue burning in China's middle–east, the r between crop residue burning spots and $PM_{2.5}$ is 0.6921 ($P<0.01$) in 2014 and 0.5620 ($P<0.01$) in 2015, while the correlation coefficient of autumn-winter crop residue burning in China's northeast is slightly lower with an r of 0.5670 ($P<0.01$) in 2014 and 0.6213 ($P<0.01$) in 2015. In autumn-winter, crop residue burning can induce evident $PM_{2.5}$ increase in China's northeast, and that is more obvious than summer crop residue burning in China's middle–east. Furthermore, when data of summer and autumn-winter crop residue burning from 2014 and 2015 are compared, we can see that the change in number of crop residue burning spots significant changes $PM_{2.5}$ in these regions. Both the summer and autumn-winter crop residue burning areas presented spatial consistency with high $PM_{2.5}$. By contrast, the results from many aspects indicated that the crop residue burning in spring did not cause a notable change of $PM_{2.5}$.

Capsule Abstract: East Central China's summer season (June) and Northeast China's autumn-winter season (October-November) both experience increase of $PM_{2.5}$, which is closely related to crop residue burning.

*Corresponding author.
E-mail address: yinshuai@env.agr.hokudai.ac.jp

Keywords: air pollution; MOD14A1; MCD12Q1; northeast China; spatial consistency.

1. Introduction

Crop residue consists of materials left over from the production of crops, including the straw (or stalks) of rice, wheat, maize, sugarcane, and cereal (Lal, 2005). How to reuse crop residue effectively at a low cost is always a disturbing problem for crop planting (Smil, 1999). In developed countries, through technological progress and innovation, the comprehensive use of crop residue has been achieved in a variety of ways. For example, in 24 agricultural states in the United States, approximately 45 million tons of wheat crop residue have been collected to make fodder, arts & crafts, and used as insulation for house construction that is a popular commercial product (Lei et al., 2007). Straw fibers, when compresses under high temperature, bond together without any adhesive. For structural applications, the strawboard is then laminated between oriented-strand board to form a stress-skin panel (Glaser and Van Dyne, 1997). In addition, the U.S. government has paid more attention to biomass energy since the mid-1990s to mitigate global climate change (Wise et. al., 2014). Crop residue is used to generate electricity in Denmark, which not only increases income for local farmers but also cuts power plant costs (Nguyen et al., 2013). In Canada and Japan, most of the crop residue is shattered directly and returned to the farmland as fertilizer (Wang, 2010). In developing countries, effective methods of crop residue reuse are also a challenge for the government. Some innovative methods, such as using crop residue to generate methane or industrial raw materials and to raise edible mushrooms, have been implemented in China (An et al, 2004). However, because of the high cost, low agricultural product price and lack of certain technologies, the comprehensive use of crop residue is very hard to generalize across the country. According to estimates, from 1995 to 2005, China produced some 630 million tons of crop residue per year, one-third of which remained unused and most of which was burnt directly in the field (Liu et al., 2008; Wang et al., 2013). The burning of crop residue emits carbon dioxide, carbon monoxide, non-methane-hydrocarbons, nitric oxide, nitrous oxide and atmospheric particles (Hayashi et al., 2014). Open crop residue burning has caused great concern recently for its significant emissions of black carbon and organic carbon (Kharol et al., 2012; Hsu et al., 2009). These emissions can result in severe degradation of regional air quality (Crounse et al., 2009) and increasing respiratory disease morbidity (Arbex and Brage, 2007).

Because of the different climatic conditions and farming modes in China, the burning of crop residue is known to be spatially and temporally inhomogeneous, requiring better characterization. While burning is dispersed across the country after harvest and lasts for a short time, it is unrealistic to monitor the burning of crop residue on the ground. Satellite remote sensing, because of its synoptic and repetitive coverage, can supply

information to characterize fires in terms of intensity, extent, spatial-temporal variations, and radioactive energy (Lentile et al., 2006). This would supply efficient data that could be used to analyze the spatial and temporal change of crop residue burning on a large scale (McCarty, 2011; Vadrevu et al., 2014).

As the largest developing country in the world, China suffers from severe air pollution, especially haze in recent decades (Madaniyazi et al., 2015). Haze is traditionally an atmospheric phenomenon where dust, smoke and other dry particles obscure the clarity of the sky (Zhang et al., 2015). Haze often occurs when dust and smoke particles accumulate in relatively dry air (Youngsin and Lim, 2014). When weather conditions block the dispersal of smoke and other pollutants, they concentrate and form a usually low-hanging shroud that impairs visibility and may become a respiratory health threat (Othman et al., 2013).

The causes of severe haze in China are still controversial. The rapid economic increase in past decades has led to a soaring consumption of fossil energy (Liu and Li, 2011). Additionally, non-point source pollutions of water and soil resources, crop residue burning, special climatic condition, land cover and topography in China are also presumed to be causes of haze. Developed countries such as the United States and England also suffer from haze due to past industrial development (Wang and Liu, 2014). However, the situation in China is different. Although the Chinese government has taken effective measures to save energy and reduce emissions (Zhou et al., 2012; Yang et al., 2013), the occurrence of haze still shows no declining trend. $PM_{2.5}$, fine particles with a diameter of 2.5 micrometers or less (Zheng et al., 2005), is the most important index by which to judge the severity of haze. $PM_{2.5}$ in China began to be monitored in 2012 only in important regions, such as Beijing, Tianjin, the Yangtze River Delta Region, the Pearl River Delta Region and provincial capitals. In 2015, monitoring was extended to every prefecture-level city, and these data provide sufficient support for the study of $PM_{2.5}$ (http://dignitaries.china.com.cn/html/huanbao/3714.html).

An adequate understanding of the relationship between crop residue burning and $PM_{2.5}$ is a prerequisite for taking effective measures to decrease the occurrence of haze in developing countries. However, due to the lack of accurate time-series data and the fact that China only began monitoring $PM_{2.5}$ in 2012, no research exists on the relationship between crop residue burning and $PM_{2.5}$. To fill this gap, the aims of this study were as follows: first, use MOD14A1 and MCD12Q1 products of MODIS to analyze the changes and distributions of crop residue burning in China in 2014 and 2015; second, use the Kriging method to analyze the spatial distribution of $PM_{2.5}$ in China in 2014 and 2015 based on daily air quality data from China's National Environmental Monitoring Center; and third, use the daily data of crop residue burning and $PM_{2.5}$ to analyze their spatial and temporal relationships.

2. Data and Methods

91 2.1. Data

92 2.1.1. MOD14A1 products

93 MODIS Thermal Anomalies/Fire products are primarily derived from MODIS bands at 4 and 11
94 micrometer radiances (http://modis.gsfc.nasa.gov/data/dataprod/mod14.php). The fire detection strategy is
95 based on absolute detection of a fire (when the fire strength is sufficient to detect) and on detection relative to
96 its background (to account for variability of the surface temperature and reflection by sunlight). Numerous tests
97 are employed to reject typical false alarm sources, such as sun glint or an unmasked coastline (Giglio et al.,
98 2003).

99 MOD14A1 is produced every 8 days at a resolution of 1 kilometer as a gridded level-3 product in the
100 Sinusoidal projection. This product is unique in that it has three dimensions: fire-mask (1D) and a maximum
101 fire-radiative-power (2D) are provided for each day (3D) in the 8-day period. For example, the fire-mask
102 contains eight, band-sequential (day) 1200 × 1200 images of fire data representing consecutive days of data
103 collection. By separating the eight fire-masks, we can attain the daily Thermal Anomalies/Fire images.

104 The area of China spans from 53°33’ N to 3°52’ N and from 73°40’E to 135°2’ E, which includes 22 tiles
105 of MODIS products. The tile numbers are h25v03, h26v03, h23v04, h24v04, h25v04, h26v04, h27v04, h23v05,
106 h24v05, h25v05, h26v05, h27v05, h28v05, h25v06, h26v06, h27v06, h28v06, h29v06, h28v07, h29v07,
107 h28v08 and h29v08. In this study, MOD14A1 products for the whole of China from 2014 and 2015 were
108 obtained from NASA’s LAADS Web (https://ladsweb.nascom.nasa.gov/data/search.html).

109 2.1.2. MCD12Q1 products

110 The MODIS Land Cover Type product provides data characterizing five global land cover classification
111 systems (Cai et al., 2014). In addition, it provides a land cover type assessment and quality-control information.
112 The primary land cover scheme identifies 17 land cover classes defined by the International Geosphere
113 Biosphere Programme (IGBP) (Loveland et al., 1997), which includes 11 natural vegetation classes, three
114 developed and mosaicked land classes, and three non-vegetated land classes. In this study Class 12 (Croplands)
115 from the primary land cover scheme was used to extract crop residue burning spots. The latest MCD12Q1, the
116 land cover from 2013, was also obtained from NASA’s LAADS Web.

117 2.1.3. $PM_{2.5}$ data

118 Daily air quality data—including $PM_{2.5}$, PM_{10}, AQI and quality grade—were obtained from China’s
119 National Environmental Monitoring Center (http://www.cnemc.cn/). China’s Environmental Protection
120 Conference of 2012 first mentioned and emphasized monitoring $PM_{2.5}$ and ozone across the country. By 2015,
121 $PM_{2.5}$ monitoring has been extended to every prefecture-level city. In this study, daily $PM_{2.5}$ data were collected

from 150 cities in 2014 and 285 cities in 2015 to analyze the $PM_{2.5}$ spatial distribution change and explore the relationship between crop residue burning and $PM_{2.5}$ change. The $PM_{2.5}$ monitor cities cover all the provinces and are mainly concentrated in China's east, which suffers from severe air pollution.

2.1.4. GIS data

The temporal resolution of both crop residue burning and $PM_{2.5}$ are well qualified at daily levels. To perform a specific analysis, it is necessary to calculate the crop residue burning spots and $PM_{2.5}$ on a provincial level. Therefore, GIS data for China, such as the boundary and area of each province and the geographic coordinates of its cities, were used in this study. The GIS data were from the newest version (November 2015) of GADM database, which is a spatial database of the location of the world's administrative areas (or administrative boundaries) for use in GIS and similar software. Administrative areas in this database are countries and lower level subdivisions such as provinces, cities, counties, and so on. GADM describes where these administrative areas are, and for each area it provides some attributes, such as the name and variant names (http://www.gadm.org/country).

2.2. Methods

2.2.1. Process for obtaining crop residue burning data

MOD14A1 was used for two main reasons: to obtain the distribution map for crop residue burning and to compile the statistics for daily and monthly crop residue burning at the provincial level. First, after collecting MOD14A1 images from 2014 and 2015 in China, we obtained daily Thermal Anomalies/Fire images by separating the eight fire-masks. Second, the cropland area of MCD12Q1 was used to clip Thermal Anomalies/Fire images to obtain the daily crop residue burning spots. Afterwards, the daily crop residue burning spots were combined with the monthly crop residue burning spots and these spots were vectorized separately. Finally, we created a fishnet of squares measuring 0.5°×0.5° to cover all of China, and, by joining the crop residue burning spots with this fishnet, we finally obtained the daily and monthly distribution map showing crop residue burning. In the meantime, by joining the crop residue burning spots with the GIS data for China, we created the statistics for crop residue burning spots on a provincial scale (Fig. 1). The resolution of MOD14A1 products is 1,000 m×1,000 m, and each pixel after the vectorization was regarded as a crop residue burning spot. All the procedures above were conducted on ERDAS, ArcGIS and ModisTool platforms.

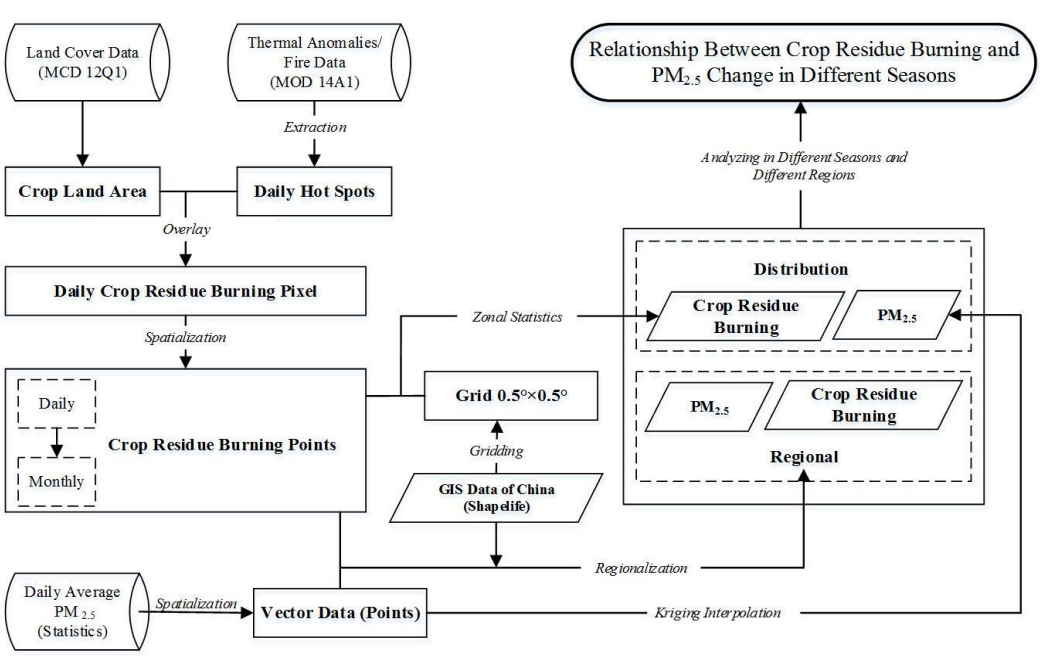

Fig. 1. Flow chart of obtaining crop residue burning data and $PM_{2.5}$ data.

2.2.2. Process for obtaining $PM_{2.5}$ data

After acquiring the daily average $PM_{2.5}$ data from China's National Environmental Monitoring Center, the data were combined with the geographic coordinates of each city. Then, the $PM_{2.5}$ data for 150 cities in 2014 and 285 cities in 2015 were converted into vector data (point shapefile), which are more suitable for mapping the $PM_{2.5}$ distribution. For the 150 cities in 2014, the minimum distance between each other is 30.52 km, maximum distance is 3803.48 km and average distance is 1195.16 km. For the 285 cities in 2015, the minimum distance between each other is 22.39 km, maximum distance is 4574.63 km and average distance is 1368.42 km. Finally, the ordinary Kriging interpolation method and the daily $PM_{2.5}$ data for 150 cities in 2014 and 285 cities in 2015 was used to obtain the $PM_{2.5}$ distribution map of China (Fig. 1). The Kriging interpolation method is an important geostatic method based on the use of a variogram (Guo et al., 2013). A variogram is a geostatistical technique that can be used to examine the spatial continuity of a regionalized variable and how this continuity changes as a function of distance and direction. Under suitable assumptions on the priors, Kriging gives the best linear unbiased prediction of the intermediate values. By using the Geostatistical Analyst on the ArcGIS platform, we can obtain the parameters (range, nugget and sill) of experimental semivariogram to perform the interpolation. In this section, the Kriging interpolation method is only used to present the spatial distribution characteristics of $PM_{2.5}$ and the regional and period $PM_{2.5}$ data are calculated with the daily average concentration from monitoring station.

After all of the processes described above, we can mainly acquire two sets of data, one is spatial distribution maps of crop residue burning and $PM_{2.5}$ concentration, the other one is regional statistic data of

crop residue burning spots and $PM_{2.5}$ concentration. Then, the temporal and spatial distribution characteristics of crop residue burning and $PM_{2.5}$ concentration were illustrated on a national scale. Furthermore, China's middle-east and northeast would be regarded as representative region to analyze the relationship between crop residue burning and $PM_{2.5}$ change and the different attributes in four seasons are also revealed.

3. Results

3.1. Monthly changes in crop residue burning in China

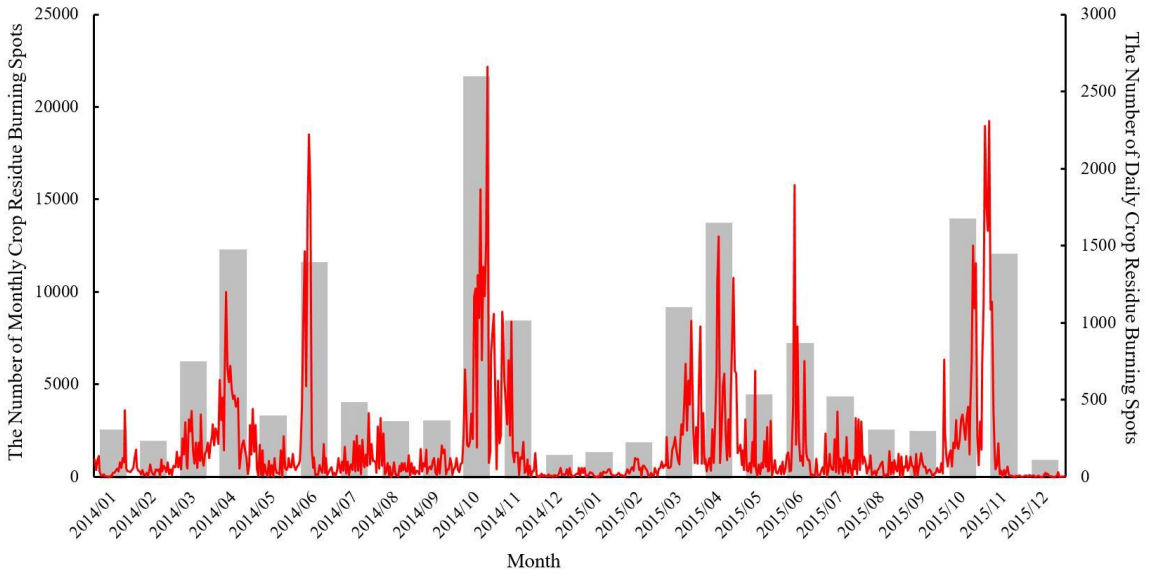

Fig. 2. The daily (red line) and monthly (gray column) number of crop residue burning spots in China.

We extracted the daily and monthly number of number of crop residue burning spots in 2014 and 2015 from MODIS products. Table 1 shows that there were 71,237 and 66,051 crop residue burning spots in 2014 and 2015, respectively. Crop residue burning spots accounted for 52.08% and 56.47% of all the hot spots from MODIS in 2014 and 2015. Meanwhile, the rations between crop residue burning spots and all hot spots in June, October and November were much higher than that in other months. As Fig. 2 and Table 1 shows, the number of spots in October was the highest of the whole year. Meanwhile, the number of monthly crop residue burning spots showed a similar change tendency in the two years studied. The monthly and daily crop residue burning spots were mainly concentrated in 3 periods: from March to April, in July and from October to November. On October 23, 2014 and November 4, 2015, the number of crop residue burning spots was 2,661 and 2,310, respectively, the highest daily totals for the two years. These days corresponded with China's autumn harvest. The second most intensive time for crop residue burning in 2014 and 2015 was on June 11, which corresponded the summer harvest time in China.

Table 1
Statistic of crop residue burning spots and all hot spots from MOD14A1 in China, China's middle–east and China's northeast

Year	Month	Whole China			China's middle–east			China's northeast		
		Crop residue burning	All hot spots	Ration (%)	Crop residue burning	All hot spots	Ration (%)	Crop residue burning spots	All hot spots	Ration (%)
2014	Jan	1886	16194	11.65	440	941	46.76	68	85	80.00
	Feb	1288	5723	22.51	42	102	41.18	523	679	77.03
	Mar	5560	14639	37.98	938	1454	64.51	2679	3781	70.85
	Apr	11628	22735	51.15	1201	1751	68.59	7890	11470	68.79
	May	2631	6453	40.77	1522	1913	79.56	239	501	47.70
	Jun	10912	13216	82.57	10338	10849	95.29	155	462	33.55
	Jul	3370	6404	52.62	1811	2291	79.05	169	532	31.77
	Aug	2324	4752	48.91	1173	1503	78.04	267	793	33.67
	Sep	2391	5473	43.69	342	489	69.94	691	1297	53.28
	Oct	20965	26282	79.77	1338	1573	85.06	17411	19296	90.23
	Nov	7767	10637	73.02	355	467	76.02	6563	7150	91.79
	Dec	515	4266	12.07	131	234	55.98	61	75	81.33
	Sum	**71237**	**136774**	**52.08**	**19631**	**23567**	**83.30**	**36716**	**46121**	**79.61**
2015	Jan	654	7402	8.84	123	258	47.67	33	51	64.71
	Feb	1187	5823	20.38	175	306	57.19	453	618	73.30
	Mar	8511	15216	55.93	781	1062	73.54	5166	6237	82.83
	Apr	13075	23541	55.54	788	1070	73.64	9751	12737	76.56
	May	3787	7436	50.93	2238	2735	81.83	507	1082	46.86
	Jun	6555	8821	74.31	5777	6223	92.83	184	547	33.64
	Jul	3652	6566	55.62	2329	2829	82.33	197	607	32.45
	Aug	1885	4473	42.14	884	1269	69.66	164	476	34.45
	Sep	1802	4085	44.11	422	560	75.36	653	1410	46.31
	Oct	13293	18997	69.97	2019	2274	88.79	9176	11396	80.52
	Nov	11397	13709	83.14	106	155	68.39	10614	11845	89.61
	Dec	253	900	28.11	105	135	77.78	63	79	79.75
	Sum	**66051**	**116969**	**56.47**	**15747**	**18876**	**83.42**	**36961**	**47085**	**78.50**

To understand the spatial characteristics of crop residue burning, we made the monthly distribution map. In March and April, burning spots are mainly distributed in China's north, especially the northeast because of straw burning before spring ploughing. During this period, local farmers burn the straw left on the farmland as fertilizer to make the spring ploughing easier. The burning spots even show a transfer trend to more northerly regions from March to April. This is consistent with spring ploughing times in China's northeast. The fire points in June are mainly distributed in the Henan, Shandong, Anhui, Jiangsu and Hebei provinces, which are China's wheat planting areas (Fang et al., 2014). In June, after the wheat harvest, a large proportion of wheat straw is burnt directly on the farmland. According to the report from China's Ministry of Environmental Protection

(http://www.zhb.gov.cn/), crop residue burning spots in June 2015 decreased by 45.35% compared with those in 2014. Meanwhile, the results of this study demonstrated a 39.93% decrease in June 2015, conforming to the official report. In October, crop residue burning spots rose to 20,965 in 2014 and 13,293 in 2015. This sudden increase was caused by autumn harvest. In October, the spots are mainly concentrated in China's northeast, and this is consistent with harvest times for corn, soybean and rice in China's north. In November, the number of crop residue burning spots showed a distinct decrease, but in China's northeast, crop residue burning was still ongoing. This is because the high latitudes result in a later harvest time in this region than in other places. In December, the number of crop residue burning spots decreased to the lowest rates in the whole year.

3.2. Monthly $PM_{2.5}$ changes in China

$PM_{2.5}$ is an important indicator of air quality, and reducing $PM_{2.5}$ effectively is key to decreasing the occurrence of haze in China. However, there is hardly any research about $PM_{2.5}$ changes in China because of the shortage of time-series $PM_{2.5}$ data. In this study, we used daily air quality data from China's National Environmental Monitoring Center to study temporal and spatial changes in $PM_{2.5}$ in China. The data show that $PM_{2.5}$ is always higher in winter than in other seasons. In January the average $PM_{2.5}$ was the highest of the year. After January, $PM_{2.5}$ declined for 9 consecutive months and finally reached in September, making it the month with the lowest $PM_{2.5}$ concentration of the year. After September, $PM_{2.5}$ grew continuously until the end of the year. The monthly $PM_{2.5}$ value was always lower in 2015 than in 2014 and the average $PM_{2.5}$ in 2015 was 54.03 $\mu g/m^3$, a decrease of 11.15% when compared with 2014. This result is in accordance with Greenpeace's report (http://www.greenpeace.org.cn/city-ranking-2015-half-year).

The $PM_{2.5}$ distribution map shows that $PM_{2.5}$ in China's east is always higher than in China's west. Dense population, cities, and rapid industrial development in China's east are the main causes of higher $PM_{2.5}$. The distribution shows that $PM_{2.5}$ in the west of the Xinjiang Uygur Autonomous Region is also higher than in other regions. That is related to poor surface conditions and low vegetation cover, causing dusty weather to be more likely to occur (Qian et al., 2007). Meanwhile, Taklimakan Desert is also located in the Xinjiang Uygur Autonomous Region (Dong et al., 2004). The result also shows that $PM_{2.5}$ in China's north is always higher than in China's south. Because China's north is far away from the ocean, dry climate and serious desertification, dusty weather is more common in this region. Moreover, most of China's energy resources and processing are distributed in its north. Mining, transportation and processing will produce massive dust and airborne particles. Coal-fired heating in the winter in China's north also exacerbates the increase of $PM_{2.5}$.

3.3. The relationship between $PM_{2.5}$ and crop residue burning

3.3.1. The relationship between $PM_{2.5}$ and crop residue burning in spring

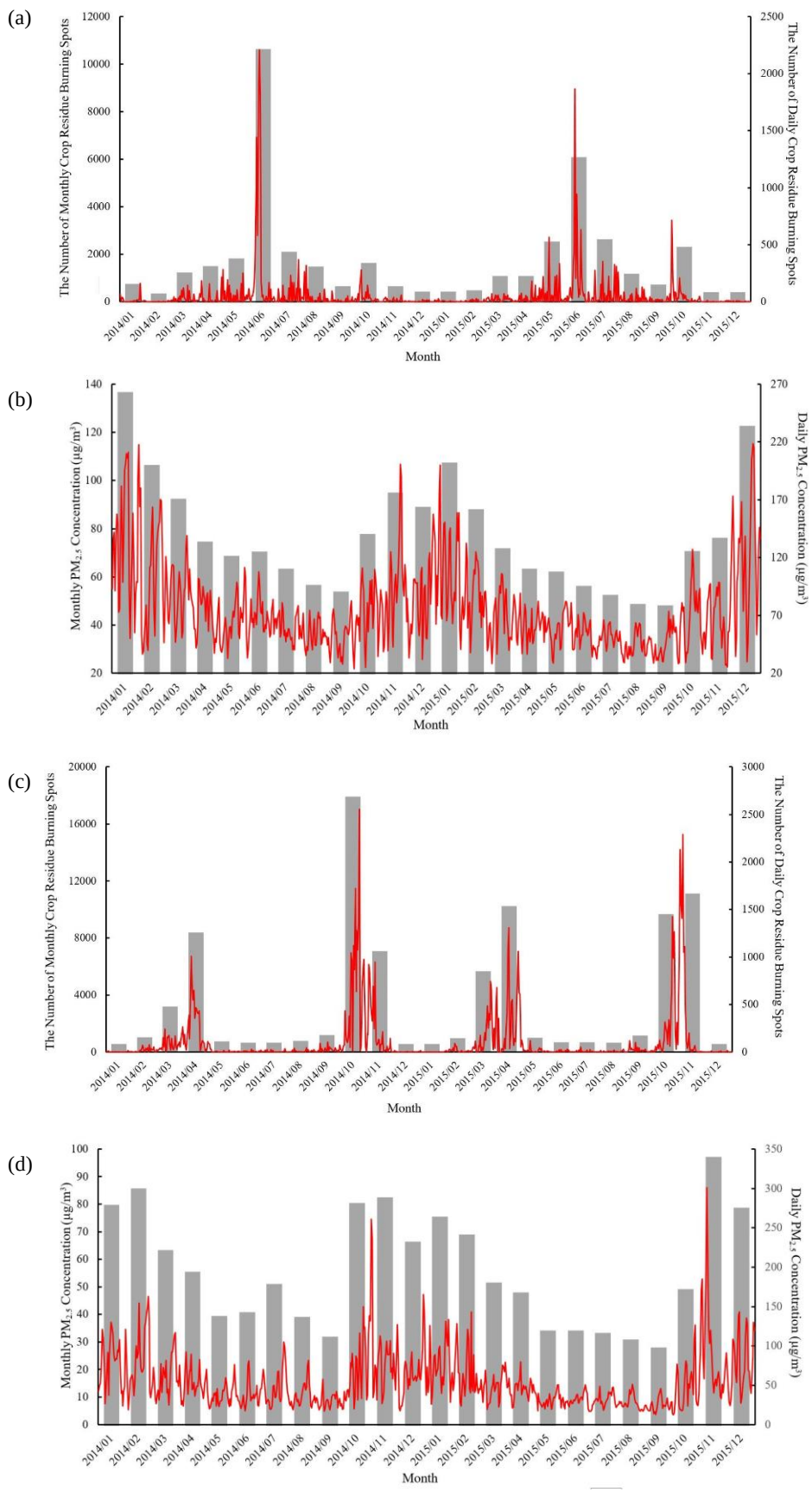

Fig. 3. The daily (red line) and monthly (gray column) data of crop residue burning spots in China's middle-east (a) and China's northeast (c) and $PM_{2.5}$ concentration in China's middle-east (b) and China's northeast (d).

Crop residue burning in the spring is mainly concentrated in China's northeast in March and April before spring ploughing. Heilongjiang Province, Jilin Province and Liaoning Province, all located in China's northeast, account for 61.46% in 2014 and 69.10% in 2015 of burning spots from the whole country in these two month. Fig. 3 also demonstrates there are two significant crop residue burning period in northeast China, one is from March to April and the other one is from October to November. Therefore, these three provinces are regarded as the study region in this section. Fig. 4 shows that, the crop residue burning is more concentrated in April than that in March and the crop residue burning spots of 3 provinces reached its highest point on April 10, 2014, and April 15, 2015, with numbers of 1,308 and 1,009, respectively. The burning time in spring was dispersive and $PM_{2.5}$ change trend was random. Unlike the crop residue burning in summer and autumn-winter, crop residue burning and $PM_{2.5}$ present different tendency and $PM_{2.5}$ did not show a notable increase after the burning of crop residue. Table 3 also demonstrates that the crop residue burning in these three provinces did not induce $PM_{2.5}$ concentration increase in certain period and it shows a stable decrease that is consistent with that of other provinces. Meanwhile, comparing the data in 2015 with 2014 (Table 2), the number of crop residue burning spots in both March and April rise evidently, with 92.83% increase in March and 23.59% increase in April. On the contrary, the concentration of $PM_{2.5}$ in March declined 19.25%, from 60.58 $\mu g/m^3$ to 48.92 $\mu g/m^3$, and for April, it declined 14.02%, from 52.70 $\mu g/m^3$ to 45.31 $\mu g/m^3$, which is even more intense than the annual $PM_{2.5}$ decrease (11.15%). Therefore, when we compare the spring residue burning data and $PM_{2.5}$ data from 2014 and 2015, we can conclude the change in crop residue burning spots did not cause an evident change in $PM_{2.5}$ that is also different from the results of crop residue burning in summer and autumn-winter. Furthermore, through analyzing the daily data of crop residue burning spots and $PM_{2.5}$, we found there was no correlation between crop residue burning and $PM_{2.5}$ on the same day or from several days later and the $PM_{2.5}$ did not present a rising tendency during the crop residue burning (Table 3). Regarding spatial distribution, even though most of the crop residue burning spots in March and April is distributed in China's northeast, the $PM_{2.5}$ concentration was very low in this region. In these two months, crop residue burning and $PM_{2.5}$ showed no spatial consistency.

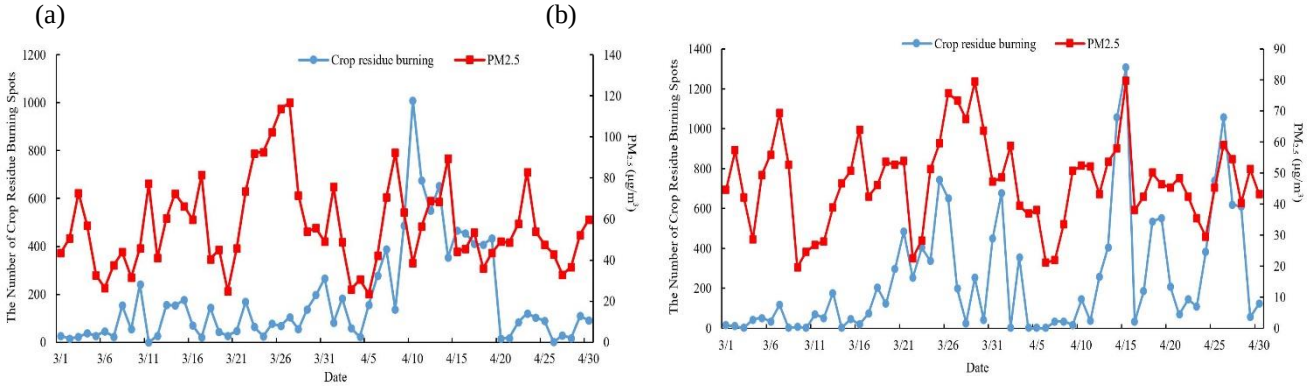

Fig. 4. The number of crop residue burning spots and $PM_{2.5}$ of China's northeast in March and April: 2014(a); 2015(b).

On the daily-level, period-level (Table 3), year-level (Table 2) and spatial distribution, all the results indicated that the crop residue burning in spring cannot cause a notable change of $PM_{2.5}$ that was totally different from the final results of summer and autumn-winter. As mentioned above, since the crop residue burning in these two month was before the spring ploughing and the other two were after the harvest of crops, the amount of biomass burnt in spring was much less that in summer and autumn-winter. However, there were large numbers of crop residue burning spots in spring, a large proportion of the crop residue had already been burned in last autumn-winter. Meanwhile, the crop residue burning time in spring was more scattered than the other two which would reduce its effects on $PM_{2.5}$ change.

Table 2
Comparing change tendency of crop residue burning spots and $PM_{2.5}$ concentration between 2014 and 2015

Month	Crop residue burning			$PM_{2.5}$ ($\mu g/m^3$)		
	2014	2015	Change ration (%)	2014	2015	Change ration (%)
March	2679	5166	92.83	60.58	48.92	-19.25
April	7890	9751	23.59	52.70	45.31	-14.02
June	10338	5777	-44.12	67.43	53.06	-21.31
October	17411	9176	-47.3	77.74	46.48	-40.21
November	6563	10614	61.72	79.81	94.38	18.26

For March, April, October and November, the study region is the three provinces in China's northeast; for June, the study region is the five provinces in China's middle-east.

3.3.2. The relationship between $PM_{2.5}$ and crop residue burning in summer

Crop residue burning in the summer is mainly concentrated in China's middle–east in early June, after the winter wheat harvest. As China's wheat production region, Henan, Shandong, Anhui, Jiangsu and Hebei provinces are all located in China's middle–east, and these five provinces account for a large proportion of crop residue burning spots in June. Crop residue burning spots in these five provinces in June constituted 94.74% of all spots in China in 2014 and 88.13% in 2015.Therefore, these five provinces are regarded as the study region for this part of the study. Fig. 3 shows that in this region the crop residue burning of June was much higher than other month and the daily number also reached peak during this period. Meanwhile, Table 1 indicates that in China's middle–east the rations between crop residue burning and all hot spots in this month were even over 90%, which were also the highest of the whole year. To the $PM_{2.5}$ concentration (Fig. 3), the month change trend was almost the same as that of the whole China. But in June 2014 the concentration was little higher than last month that is different from the whole China. The daily data (Fig. 5) shows that crop residue burning and $PM_{2.5}$ present similar change tendency, but the change in $PM_{2.5}$ is delayed by approximately 4 days. Crop residue

burning in the summer lasts for approximately 1 week: for 2014 that was from June 5 to 14, and for 2015, that was from June 9 to 15. Crop residue burning in these 5 provinces reached its highest point on June 11 for both years, with the number of spots registering at 2,210 in 2014 and 1,866 in 2015. After the peak of crop residue burning, $PM_{2.5}$ started to show a growth trend and finally reached its highest point 4 days later in China's middle–east. $PM_{2.5}$ reached its highest point on June 15 of both years, with values of 116.76 μg/m^3 in 2014 and 86.70 μg/m^3 in 2015, showing a decrease of 30.06 μg/m^3 between the years. Moreover, when compared with 2014, the annual decrease of $PM_{2.5}$ in 2015 was 11.15%. Meanwhile, $PM_{2.5}$ in June in these 5 provinces deceased 21.31% from 67.43 μg/m^3 in 2014 to 53.06 μg/m^3 in 2015 (Table 2), a more intensive decrease than the annual decrease. Table 2 also shows that crop residue burning spots in June 2015 presented a 44.12% decrease from previous year. Therefore, this finding indicates the decrease in crop residue burning is consistent with the decline in $PM_{2.5}$ in June, the summer harvest month. And the efforts of local government to reduce crop residue burning and improve air quality have achieved remarkable results. Meanwhile, Table 3 demonstrates that the crop residue burning in these five provinces induced $PM_{2.5}$ concentration increase during crop burning time, after that $PM_{2.5}$ concentration presented a steep fall that is totally different from the result of other provinces which showed a stable decline during this period. In June 2015, as the crop residue burning spots dropped from previous year, the $PM_{2.5}$ concentration increase in burning time was not so evident.

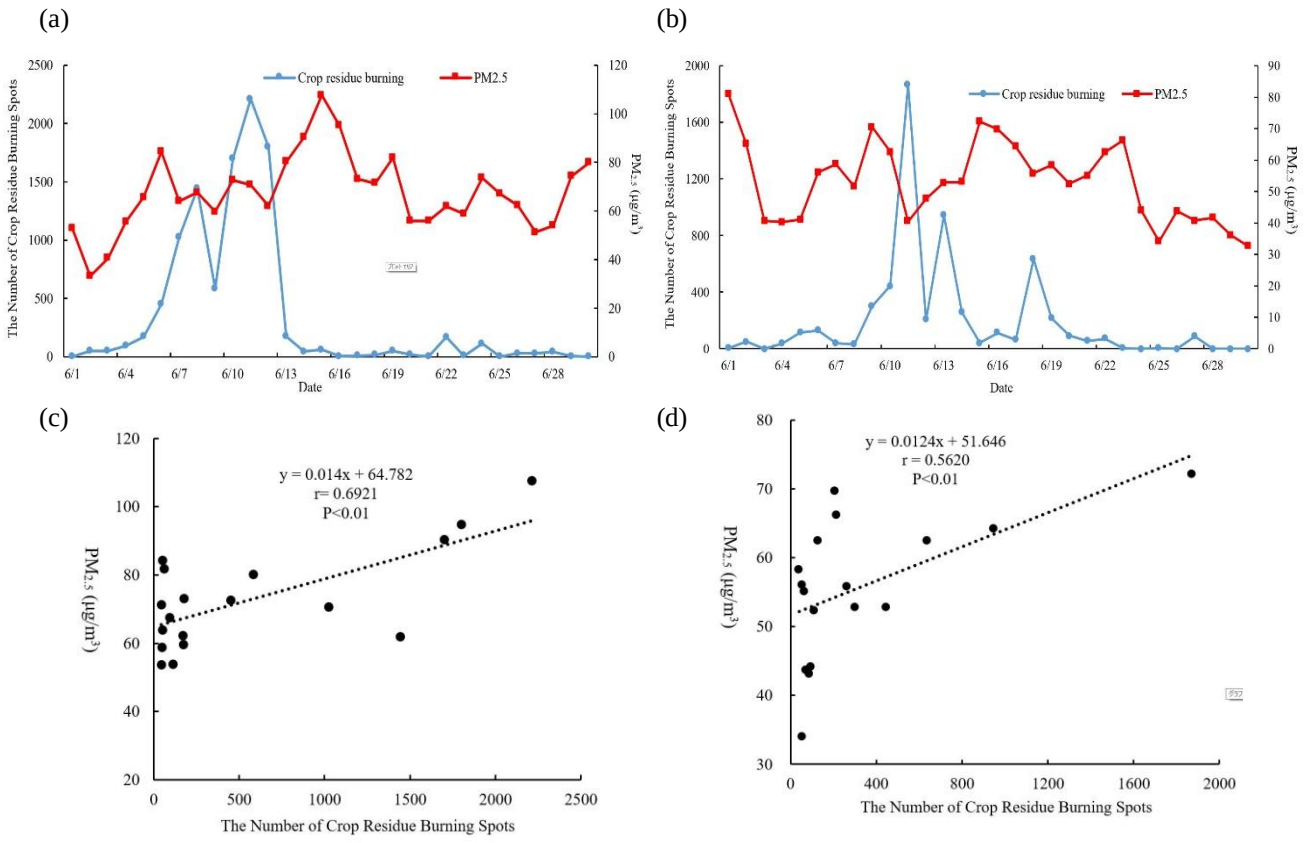

Fig. 5. The number of crop residue burning spots and $PM_{2.5}$ of China's middle–east in June: 2014(a); 2015(b). And the correlation between the number of crop residue burning spots and $PM_{2.5}$ measured 4 days later: June 2014(c); June 2015(d).

In these five provinces with an area of 759,400 km^2, crop residue burning cannot induce an instantaneous increase in $PM_{2.5}$. Therefore, there is no correlation between crop residue burning and $PM_{2.5}$ on the same day. In 2014 and 2015, the crop residue burning in other provinces (excluding the five provinces in China's middle–east and three provinces in China's northeast) was not severe and the average daily crop residue burning spots in these provinces would be regarded as the baseline in the daily analysis, the number of which was 38.68. If the number of average daily crop residue burning spots is below 38.68, it would be ignored, because the crop residue burning in these days is not significant. We analyzed the correlation between the number of crop residue burning spots and the $PM_{2.5}$ concentration from several days later and the final results (Fig. 5) shows that the correlation coefficient between crop residue burning and $PM_{2.5}$ from 4 days later is considerably higher with an r of 0.6921 ($P<0.01$) in 2014 and 0.5620 ($P<0.01$) in 2015. Furthermore, Fig. 5 also demonstrates that crop residue burning and $PM_{2.5}$ are positively correlated. Regarding spatial distribution, Fig. 6 shows that crop residue burning was distributed mainly in the middle–east of China in June, and $PM_{2.5}$ concentration was also high in these regions. In June 2015, crop residue burning and $PM_{2.5}$ showed higher spatial consistency, except in the west of the Xinjiang Uygur Autonomous Region. High $PM_{2.5}$ in Xinjiang is caused by its special landscape, as described earlier. In June 2014, crop residue burning was much more intensive than it was 2015. Therefore, Fig. 6 indicates that crop residue burning caused high $PM_{2.5}$ not only in and but also around those areas in this year, such as Hubei and Hunan. In summer, China's east is influenced by southeast monsoon, which is from ocean to continent, but impeded by Taihang Mountains, Qinling Mountains, Yunnan-Gzuihou Plateau and hilly region of Southeastern China, the $PM_{2.5}$ from crop residue burning can only concentrate in North China Plain and Yangtze Plain. Areas west of the Xinjiang Uygur Autonomous Region did not present high $PM_{2.5}$ in 2014 because at that time there was no $PM_{2.5}$ detection data in that area.

Table 3
$PM_{2.5}$ concentration change trend (before, during and after crop residue burning) in study region and other provinces

Year	Area	Spring(μg/m^3)			Summer(μg/m^3)			Autumn-winter(μg/m^3)		
2014	*Period*	*3/15-4/04*	*4/05-4/25*	*4/26-5/16*	*5/21-6/04*	*6/05-6/19*	*6/20-7/04*	*9/06-10/11*	*10/12-11/16*	*11/17-12/22*
	Study region	65.03	55.99	36.45	70.48	76.42	64.44	37.30	84.58	64.43
	Other provinces	68.05	58.85	46.52	44.59	42.99	32.38	48.09	61.71	68.43
2015	*Period*	*3/20-4/11*	*4/12-5/04*	*5/05-5/27*	*5/28-6/08*	*6/09-6/20*	*6/21-7/02*	*9/26-10/20*	*10/21-11/14*	*11/15-12/09*
	Study region	49.07	45.06	31.30	58.00	58.34	45.33	36.85	102.90	58.17
	Other provinces	46.32	45.73	43.29	30.38	29.48	28.81	46.49	48.71	52.77

The study region in spring and autumn-winter is China's northeast and in summer is China's middle-east. Because the $PM_{2.5}$ presented a hysteresis change, after the concentrated crop residue burning time five more days would be considered as crop residue burning period. The number of the days before, during and after crop residue burning is the same.

Overall, on the daily-level (Fig. 5), period-level (Table 3), year-level (Table 2) and spatial distribution (Fig. 6), all the results indicated that the crop residue burning of summer can induce $PM_{2.5}$ increase in China's middle-east. Although summer crop residue burning dramatically declined in 2015, the quantity is still large. For better air quality, the government needs to continue taking effective measures to reduce crop residue burning.

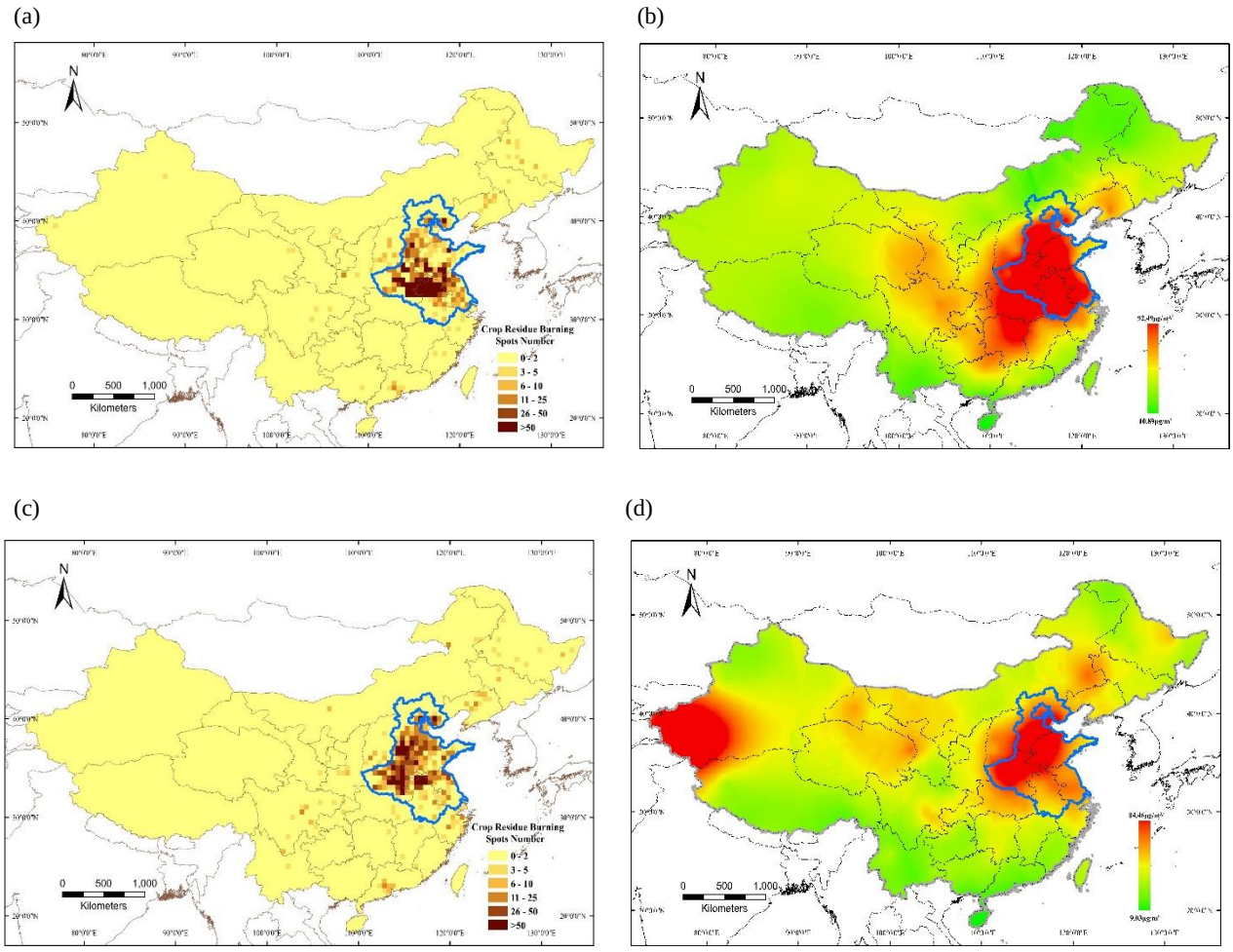

Fig. 6. Spatial distribution of crop residue burning and $PM_{2.5}$ in China in June (blue line is the boundary of the five provinces in China's middle–east): crop residue burning in June 2014(a); crop residue burning in June 2015(c); $PM_{2.5}$ distribution in June 2014(b); $PM_{2.5}$ distribution in June 2015(d).

3.3.3. The relationship between $PM_{2.5}$ and crop residue burning in autumn-winter

Autumn crop residue burning is mainly concentrated in China's northeast from late October to early November after the harvest of corn, rice and soybean. Heilongjiang Province, Jilin Province and Liaoning Province, as China's main grain producing areas, are all located in China's northeast. According to the statistics, the autumn-winter crop residue burning spots in these three province account for 83.44% in 2014 and 80.15% in 2015 of burning spots from the whole country. Therefore, these three provinces are regarded as the study region in this section. Fig. 3 shows that in this region the crop residue burning of October and November was much higher than other months and the daily number also reached peak during this period. Meanwhile, Table 1

indicates that in China's northeast the rations between crop residue burning and all hot spots in these months were around 90%, which were also the highest of the whole year in this region. To the $PM_{2.5}$ concentration (Fig. 3), the month change trend was almost the same as that of the whole China. Fig. 7 shows that crop residue burning and $PM_{2.5}$ present almost the same change tendency, with $PM_{2.5}$ delayed by several days, in accordance with the result of crop residue burning in summer. While summer crop residue burning lasts only for one week, autumn crop residue burning lasts for a longer time, approximately 1 month. In 2014, autumn crop residue burning occurred from October 12–November 11. In 2015, autumn crop residue burning was more concentrated, happening from October 21–November 9. Fig. 7 shows that crop residue burning in these 3 provinces reached its highest point on October 23, 2014, and November 4, 2015, with numbers of 2,555 and 2,291, respectively. Several days later, after the peak of crop residue burning, $PM_{2.5}$ also reached its highest point, 249.06 $\mu g/m^3$ on October 31, 2014 and 298.40 $\mu g/m^3$ on November 8, 2015, an increase of 49.34 $\mu g/m^3$ within a year. Table 2 shows that in October crop residue burning spots in these 3 provinces decreased from 17,411 in 2014 to 9,176 in 2015, a proportion of 47.30%. At the same time, $PM_{2.5}$ in October in these 3 provinces also showed a 40.21% decline from 77.74 $\mu g/m^3$ in 2014 to 46.48 $\mu g/m^3$ in 2015, while the annual decrease of $PM_{2.5}$ in all of China was only 11.15%. In November, crop residue burning spots in these 3 provinces increased from 6,563 in 2014 to 10,614 in 2015, or 61.72%. Although the annual $PM_{2.5}$ of China decreased by 11.15%, $PM_{2.5}$ in November in these 3 provinces increased 18.26% from 79.81 $\mu g/m^3$ in 2014 to 94.38 $\mu g/m^3$ in 2015. Therefore, when we compare the summer residue burning data and $PM_{2.5}$ data from 2014 and 2015, we can conclude in summer and autumn-winter the change in crop residue burning spots caused an evident change in $PM_{2.5}$. Meanwhile, Table 3 also demonstrates that during the crop residue burning time, $PM_{2.5}$ concentration in these three provinces rose dramatically, for 2014 it increased from 37.30 $\mu g/m^3$ to 84.58 $\mu g/m^3$ and for 2015 it increased from 36.85 $\mu g/m^3$ to 102.90 $\mu g/m^3$, which was more intense than other provinces. After that $PM_{2.5}$ concentration in this region presented a steep fall, while other provinces showed a stable increase during this period. These results have indicated that during the crop residue burning, the $PM_{2.5}$ in autumn-winter presented a more evident increase than that in summer. This can be explained from three aspects. Firstly, in summer the burnt crop residue was mainly from wheat stalk, while, in autumn-winter the corn stalk took a large proportion of crop residue burning. Obviously, the biomass from corn stalk is much larger than that from wheat stalk, which means more $PM_{2.5}$ release. Secondly, in autumn-winter, because of the special weather condition, thermal inversion layer is much easier to form that impede the vertical movement of air convection. This causes the pollutant near the surface, such as $PM_{2.5}$, cannot diffuse in a short time. Thirdly, except crop residue burning, there are more sources increasing the concentration of $PM_{2.5}$ in autumn- winter, including greater fossil energy consumption.

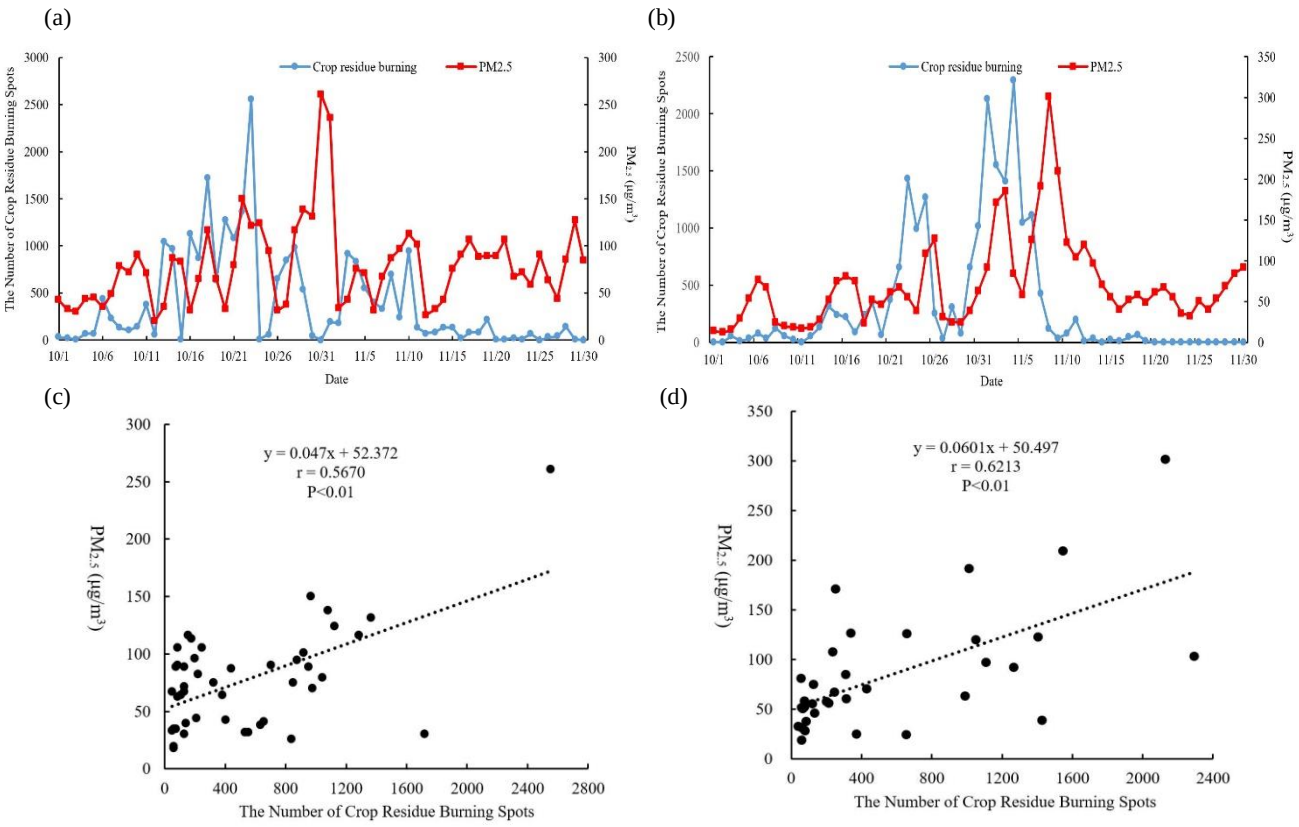

Fig. 7. The number of crop residue burning spots and $PM_{2.5}$ in China's northeast in October and November: 2014(a); 2015(b). And the correlation in China's northeast between the number of autumn crop residue burning spots and $PM_{2.5}$ from 8 days later in October and November 2014(c) and 7 days later in October and November 2015(d).

Because of the large area in China's northeast, there is no correlation between autumn crop residue burning and $PM_{2.5}$ on the same day, similar to summer crop residue burning. As mentioned before, if the number of average daily crop residue burning spots is below 38.68, it would be ignored in the daily analysis. We analyzed the correlation between the number of crop residue burning spots and the $PM_{2.5}$ concentration from several days later and the final results (Fig. 7) shows that the correlation coefficient between 2014 autumn crop residue burning and $PM_{2.5}$ from 8 days later is much higher, with r of 0.5670 ($P<0.01$). In 2015, the r between autumn crop residue burning and $PM_{2.5}$ from 7 days later was 0.6213 ($P<0.01$). Compared with summer crop residue burning, the correlation coefficient of autumn crop residue burning is lower because crop residue burning in summer was only concentrated for one week. However, the crop residue burning time in autumn is more scattered and can last for approximately one month. Even the correlation coefficient of autumn-winter crop residue burning in 2015 is higher than it was in 2014, again because of the more concentrated burning time in 2015. Additionally, the causes of $PM_{2.5}$ change in autumn and winter are more complex than in summer. Fig. 7 also demonstrates that crop residue burning and $PM_{2.5}$ are positively correlated. In summer, crop residue burning shows a higher correlation with $PM_{2.5}$ from 4 days later, while in autumn, crop residue burning demonstrates a

higher correlation with $PM_{2.5}$ from approximately 1 week later. The superposition of many factors cause this longer hysteresis in autumn-winter. As mentioned above, the formation of thermal inversion layer reduces the height of atmospheric convective boundary layer, which inhibits the vertical diffusion of pollutants. Meanwhile, without the disturbance of strong cold air during this period, the continued weak or static wind weather impedes horizontal diffusion of pollutants. These two reasons have provided sufficient conditions for pollutant accumulation. Therefore, the $PM_{2.5}$ from crop residue burning cannot diffuse in a short time. Meantime, $PM_{2.5}$ from other sources, such as vehicle exhaust and coal-fired heating, adding the $PM_{2.5}$ from crop residue burning gradually accumulate and finally reach the peak several days later.

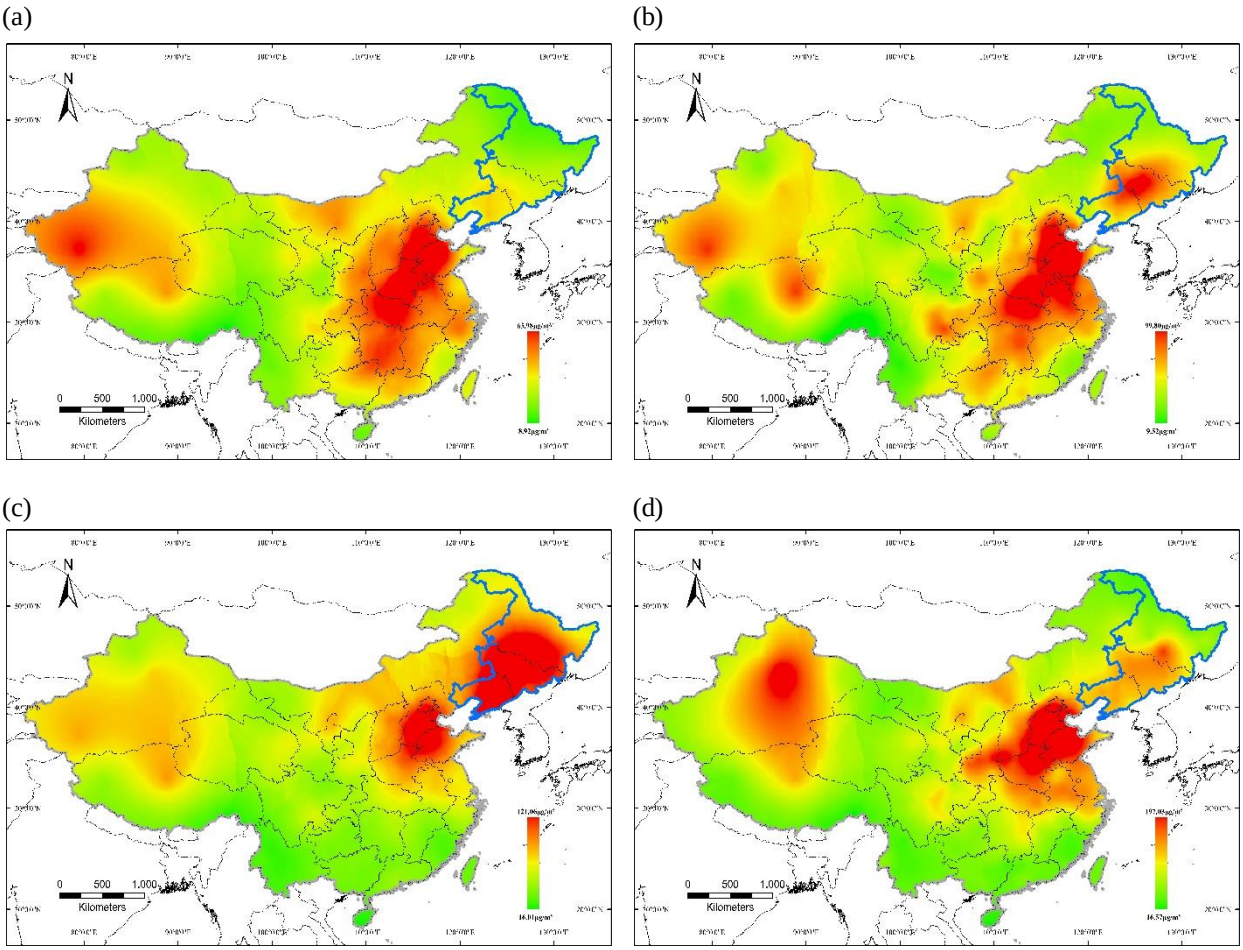

Fig. 8. Spatial distribution of $PM_{2.5}$ from September to December in 2015: September (a); October (b); November (c); December (d) (blue line is the boundary of the 3 provinces in China's northeast).

As shown in Fig. 8, the $PM_{2.5}$ of China's northeast in September is much lower than in other regions, where it is only 29.18 μg/m^3 in 2014 and 25.33 μg/m^3 in 2015, and the average $PM_{2.5}$ for China in September is 39.73 μg/m^3 in 2014 and 36.39 μg/m^3 in 2015. Fig. 8 demonstrates that in October, the $PM_{2.5}$ in China's northeast shows an increasing trend, and the $PM_{2.5}$ rises to 77.74 μg/m^3 in 2014 and 46.48 μg/m^3 in 2015. Compared with September, the speed of $PM_{2.5}$ increase in China's northeast is much faster than in other regions,

especially in 2014. Meanwhile, Fig. 9 shows that autumn crop residue burning has started in October and is mainly concentrated in China's northeast. In November, $PM_{2.5}$ remains elevated in China's northeast, at 79.81 $\mu g/m^3$ in 2014 and 94.38 $\mu g/m^3$ in 2015, which is much higher than average $PM_{2.5}$ in China in this month. At the same time, Fig. 9 shows crop residue burning is still ongoing in China's northeast. In December, average $PM_{2.5}$ across the country is increasing. By contrast, there is hardly any crop residue burning in this month, and $PM_{2.5}$ in China's northeast decreased to 63.73 $\mu g/m^3$ in 2014 and 76.05 $\mu g/m^3$ in 2015. From September to December, the change in $PM_{2.5}$ in China's northeast is consistent with crop residue burning in this area. Furthermore, crop residue burning and $PM_{2.5}$ show high spatial consistency in this area.

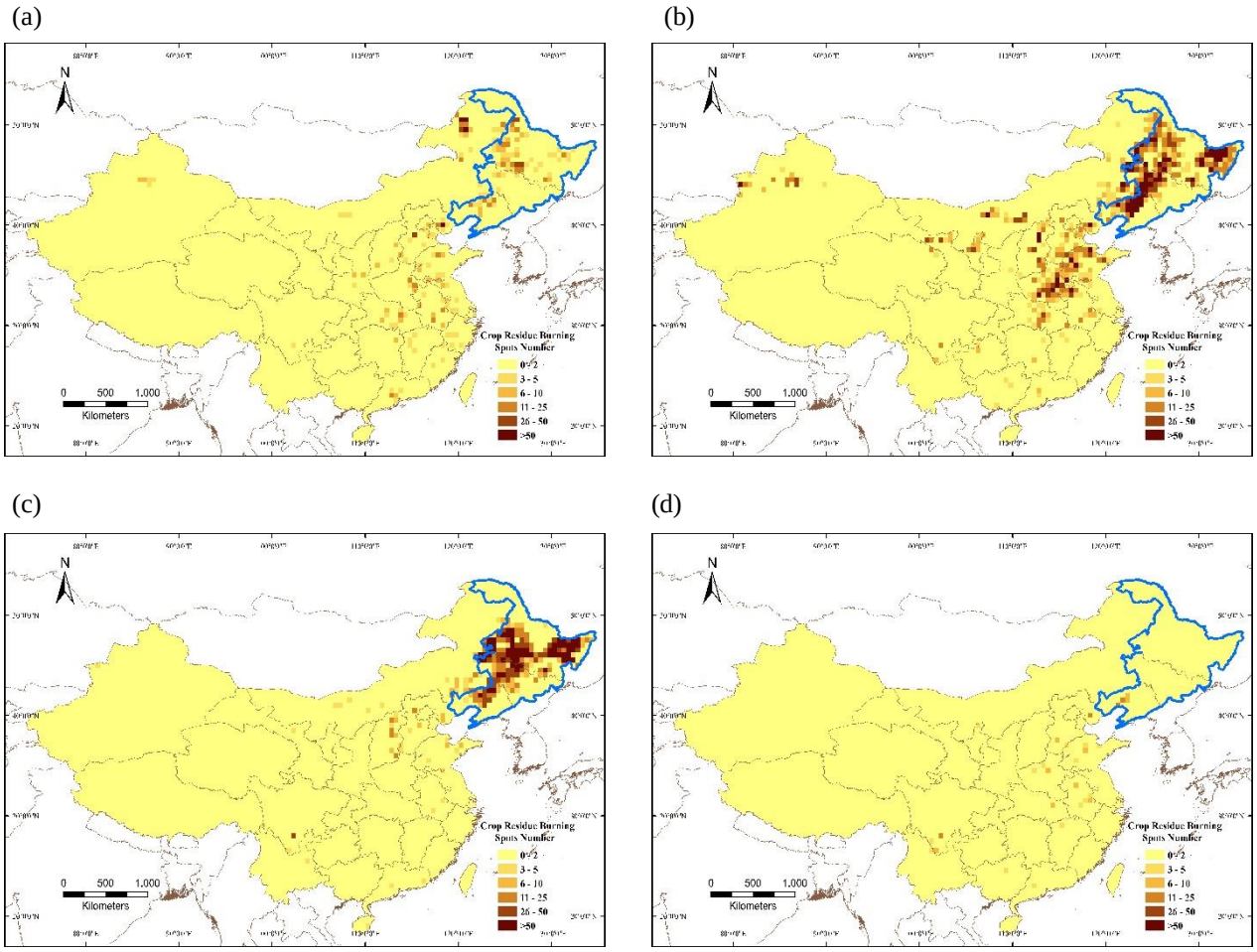

Fig. 9. Spatial distribution of crop residue burning from September to December in 2015: September (a); October (b); November (c); December (d) (blue line is the boundary of the 3 provinces in China's northeast).

Therefore, on the daily-level (Fig. 7), period-level (Table 3), year-level (Table 2) and spatial distribution (Fig. 8), all the results indicated that the crop residue burning in autumn-winter can cause a rise in $PM_{2.5}$. Compared with summer crop residue burning in China's middle–east, $PM_{2.5}$ increase of autumn-winter crop residue burning in China's northeast is more obvious.

4. Conclusions and discussions

For China and other developing countries, it is important to understand the features and relationships between crop residue burning and $PM_{2.5}$. In this study, we used MODIS products to extract the daily and monthly crop residue burning in China from 2014 to 2015, and spatial distribution was also analyzed. Meanwhile, daily air quality data were used to map the spatial distribution of $PM_{2.5}$ concentration. Finally, relationships between crop residue burning and $PM_{2.5}$ were specifically analyzed in different seasons. The main findings are listed below.

First, the spatial distribution of crop residue burning presents strong seasonal patterns in China. In summer, it mainly concentrates in China's middle–east, and in spring and autumn-winter it mainly concentrates in China's northeast. These patterns are closely related to local farming activities.

Second, $PM_{2.5}$ is always higher in winter than in other seasons, and the average $PM_{2.5}$ of 2015 decreased 11.15% compared with the previous year. Regarding $PM_{2.5}$ spatial distribution, $PM_{2.5}$ in China's east and north is higher than in China's west and south because of different anthropogenic activities, climate and landscape.

Third, crop residue burning is close related to $PM_{2.5}$ change in summer, China's middle-east and autumn-winter, China's northeast, they showed a spatial consistency during these two periods. But the crop residue burning in spring does not cause a notable change in $PM_{2.5}$. In autumn-winter, crop residue burning can effectively induce the $PM_{2.5}$ increase in China's northeast, and it is more obvious than summer crop residue burning because of the special weather condition, different crop residue and other sources of $PM_{2.5}$.

In this study, because of the high-temporal-resolution of MODIS, we can obtain the daily number of crop residue burning spots to judge the intensity of crop residue burning. But the spatial resolution of MOD14A1 is only 1 kilometer. For each pixel of crop residue burning, it only means there is crop residue burning within the 1 km^2 area and it does not represent the entire 1 km^2 area burned. If we using the area of corresponded pixel to represent the crop residue burning area the result would likely be overestimated. Therefore, in this study we cannot acquire the accurate area of crop residue burning, which is also an important index to assess the intensity of crop residue burning and the emissions. Given current satellite data characteristics, it would be hard to achieve high-spatial-resolution and high-temporal-resolution at the same time. Another important index to assess the intensity of crop residue burning is the amount of burnt biomass and the result of crop residue burning in spring have proved only the number of crop residue burning spots cannot represent the intensity of crop residue burning. Regarding the number of crop residue burning spots, some anthropogenic activities may slightly affect the final results. For example, in rural China, most of the cemeteries are dispersed on the farmland and Chinese have the tradition to show their respect to dead people by burn joss paper and paper making stuff. Addition to that, some people directly burn household garbage in the farmland. All these maybe falsely regarded

as crop residue burning. But it would not impact the accuracy of the whole results, because it is individual activity and last for a short time which is not so easy for the satellite to capture these points. From Fig. 3, the number of crop residue burning spots present different change pattern in China's middle–east and China's northeast. For China's middle–east, the crop residue burning in June is the highest of the whole year and for China's northeast, the crop residue burning in March-April and October-November is much higher than other months. The results conform to the actual situation on these two regions, which prove the final results are adequately accurate. The results about the monthly spatial distribution of crop residue burning on the whole China furtherly confirm this point.

To the $PM_{2.5}$, a variety of factors can increase its concentration. Only crop residue burning was taken into consideration in this study. For future work, more factors need to be considered to understand fully $PM_{2.5}$ change, such as vehicle emissions, coal consumption, construction dust, etc. Although annual $PM_{2.5}$ in China has decreased from 2014 to 2015, $PM_{2.5}$ is still higher than standards set by WHO (World Health Organization). Therefore, to reduce $PM_{2.5}$ emissions and control crop residue burning, China's national and local governments need to take more measures to promote the comprehensive use of crop residue.

Acknowledgments:

This work was supported by the National Natural Science Foundation of China (NO. 41301654).

References

Arbex, M.A., Brage, A.L.F., 2007. Evidence based public health policy and practice: air pollution from biomass burning and asthma hospital admissions in a sugar cane plantation area in Brazil. J. Epidemiol. Commun. H. 61, 395-400.

An, C.L., Du, J., Yue, X.Q., Zhao, J.X., 2004. Analysis on pathway of high utilization efficiency of crop stalk. China Resour. Compr. Util. 1, 25-27. DOI: 10.3969/j.issn.1008-9500.2004.01.014

Cai, S., Liu, D., Sulla-Menash, D., Friedl, M.A., 2014. Enhancing MODIS land cover product with a spatial-temporal modeling algorithm. Remote Sens. Environ. 147, 243-255.

Crounse J.D., Decarlo, P.F., Blake, D.R., Emmons, L.K., Campos, T.L., 2009. Biomass burning and urban air pollution over the Central Mexican Plateau. Atmos. Chem. Phys. 9, 2699-2734.

China National Environmental Monitoring Center. http://www.cnemc.cn/ (accessed 2015.12.20).

Dong, Z., Chen, G., He, X., Han, Z., Wang, X., 2004. Controlling blown sand along the highway crossing the Taklimakan Desert. J. Arid Environ. 57, 329-344.

Executive meeting of the State Council chaired by Premier Wen Jiabao on February 29, which agreed on the newly revised "Ambient Air Quality Standards". http://dignitaries.china.com.cn/html/huanbao/3714.html (accessed 2016.07.10).

Fang, S.B., Qi, Y., Han, G.J., Zhou, G.S., Davide, C., 2014. Meteorological drought trend in winter and spring from 1961 to 2010 and its possible impacts on wheat in wheat planting area of China. Sci. Agric. Sin. 47, 1754-1763. DOI: 10.3864/j.issn.0578-1752.2014.09.010

620 Guo, M., Wang, X.F., Li, J., Yi, K.P., Zhong, G.S., Wang, H.M., Tani, H., Schnersing, O., Reuter, M., 2013. Spatial
621 distribution of greenhouse gas concentration in arid and semi-arid region: A case study in East Asia. J. Arid Environ. 91,
622 119-128.
623 Giglio, L., Descloitres, J., Justice, C.O., Kaufman, Y.J., 2003. An enhanced contextual fire detection algorithm for MODIS.
624 Remote Sens. Environ. 87(2-3), 273-282.
625 Glaser, L., Van Dyne, D., 1997. Straw and kenaf make inroads in building materials and paper. Industrial Uses of
626 Agricultural Materials Situation and Outlook Report, IUS-7, USDA, ERS, July, 17-25.
627 Greenpeace China. $PM_{2.5}$ half-yearly report of China in 2015. http://www.greenpeace.org.cn/city-ranking-2015-half-year
628 (accessed 2016.02.05).
629 Global Administrative Areas (GADM). http://www.gadm.org/country (accessed 2015.12.8).
630 Hayashi, K., Ono, K., Kajiura, M., Sudo, S., Yonemura, S., Fushimi, A., Saitoh, K., Fujitani, Y., Tanabe, K., 2014. Trace
631 gas and particle emissions from open burning of three cereal crop residues: Increase in residue moistness enhances emissions
632 of carbon monoxide, methane, and particulate organic carbon. Atmos. Environ. 95, 36-44.
633 Hsu, N.H., Wang, S.L., Lin, Y.C., Sheng, G.D., Lee, J.F., 2009. Reduction of Cr (VI) by crop-residue-derived black carbon.
634 Environ. Sci. Technol. 43, 8801-8806.
635 Kharol S.K., Badarinath, K.V.S., Sharma, A.R., Mahalakshmi, D.V., Singh, D., Prasad, V.K., 2012. Black carbon aerosol
636 variations over Patiala city, Punjab India—A study during agriculture crop residue burning period using ground
637 measurements and satellite data. J. Atmos. Sol-terr. Phy. 84-85, 45-51.
638 Liu, W., Li, H., 2011. Improving energy consumption structure: A comprehensive assessment of fossil energy subsidies
639 reform in China. Energy Policy. 39, 4134-4143.
640 Liu, H., Jiang, G.M., Zhuang, H.Y., Wang, K.J., 2008. Distribution, utilization structure and potential of biomass resources
641 in rural China: With special references of crop residues. Renew. Sust. Energy Rev. 12, 1402-1418.
642 Lentile, L.B., Holden, Z.A., Smith, A.M.S., 2006. Remote sensing techniques to assess active fire characteristics and post-
643 fire effects. Int. J. Wildland Fire 15, 319-345.
644 Lei, D., Xi, L.W., Li, W.Z., Liu, C., 2007. Analysis on the comprehensive utilization of crop residue in foreign countries
645 Mod. Agric. Equip. 7, 67-68. http://d.wanfangdata.com.cn/Periodical/guangdnj200707034
646 Lal, R., 2005. World crop residues production and implication of its use as a biofuel. Environ. Int. 31, 575-584.
647 Loveland, T.R., Belward, A.S., 1997. The International Geosphere Biosphere Programme Data and Information System
648 global land cover data set (DISCover). Acta Astronaut 41, 681-689.
649 NASA's LAADS Web. https://ladsweb.nascom.nasa.gov/data/search.html (accessed 2015.11.6).
650 Madaniyazi, L., Nagashima, T., Guo, Y., Yu, W., Tong, S., 2015. Projecting fine particulate matter-related mortality in east
651 China. Environ. Sci. Technol. 49, 11141-11150.
652 McCarty, J.L., 2011. Remote sensing-based estimates of annual and seasonal emission from crop residue burning in the
653 contiguous United States. J. Air Waste Manage. Assoc. 61(1), 22-34.
654 Ministry of Environmental Protection of the People`s Republic of China. http://www.zhb.gov.cn/ (accessed 2015.11.12).

655 MODIS Thermal Anomalies/ Fire Products. http://modis.gsfc.nasa.gov/data/dataprod/mod14.php (accessed 2015.11.03).
656 Nguyen, T.L.Y., Hermansen, J.E., Mogensen, L., 2013. Environmental performance of crop residues as an energy source
657 for electricity production: The case of wheat straw in Denmark. Appl. Energy 104, 633-641.
658 Othman, K.A., Li, N., Abdullah, E.H., Hamzah, N., 2013. Haze monitoring system in city of Kuala Lumpur using Zigbee
659 wireless technology implementation. Proceedings of the World Congress on Engineering 2013, London, U.K, 3-5 July,
660 2013.
661 Qian, Y.B., Wu, Z.N., Yang, Q., Zhang, L.Y., Wang, X.Y., 2007. Ground-surface conditions of sand-dust event occurrences
662 in the southern Junggar Basin of Xinjiang, China. J. Arid Environ. 70, 49-62.
663 Smil, V., 1999. Crop residues: agriculture`s largest harvest: crop residues incorporate more than half of the world`s
664 agricultural phytomass. Bioscience 49, 299-308.
665 Vadrevu, K.P., Lasko, K., Giglio, L., Justice, C., 2014. Analysis of Southeast Asian pollution episodes during June 2013
666 using satellite remote sensing datasets. Environ. Pollut. 195, 245-256.
667 Wang, K., Liu, Y., 2014. Can Beijing flight with haze? Lessons can be learned from London and Los Angeles. Nat. Hazards
668 72, 1265-1274.
669 Wise, M.A., Mcjeon, H.C., Calvin, K.V., Clarke, L.E., Kyle, G.P., 2014. Assessing the interactions among U.S. climate
670 policy, Biomass Energy, and Agricultural Trade. Energy J. 35, 243-257.
671 Wang, X., Yang, L., Steinberger, Y., Liu, Z., Liao, S., Xie, G., 2013. Field crop residue estimate and availability for biofuel
672 production in China. Renew. Sust. Energy Rev. 26(6), 864-875.
673 Wang, Y.F., 2010. Analysis on the cost of applying mechanized straw returning technology. Jiangsu Agric. Mech. 6, 49-50.
674 http://d.wanfangdata.com.cn/Periodical/jsnjh201006023
675 Youngsin, C., Lim, J.Y., 2014. The recent characteristics of Asian dust and haze events in Seoul, Korea. Meteorol. Atmos.
676 Phys. 87, 143-152.
677 Yang, Z., Wang, W., Bao, H., Kong, L., Yu, B., 2013. Transport turnover with spatial econometric perspective under the
678 energy conservation and emissions reduction in China. Math. Probl. Eng. 5, 1-9.
679 Zhang, J.J., Cui, M.M., Fan, D., Zhang, D.S., Lian, H.X., 2015. Relationship between haze and acute cardiovascular,
680 cerebrovascular, and respiratory diseases in Beijing. Environ. Sci. Pollut. Res. Int. 22, 3920-3925.
681 Zhou, Z.H., Tan, Z.C., Yang, G.Q., Qiu, S.M., 2012. The study on community energy planning and emission reduction in
682 China. Adv. Mater. Res. 433-440(6), 1442-1446.
683 Zheng, M., Salmon, L.G., Schauer, J.J., Zeng, L., Kiang, C.S., Zhang, Y., Cass, G.R., 2005. Seasonal trends in PM2.5 source
684 contribution in Beijing, China. Atmos. Environ. 39, 3967-3976.